The influence of non-magnetocaloric properties on the AMR performance

Nielsen, Kaspar Kirstein; Bahl, Christian; Smith, Anders; Engelbrecht, Kurt; Olsen, Ulrik Lund; Pryds, Nini

Published in:
Proceedings of the fifth IIF-IIR International Conference on Magnetic Refrigeration at Room Temperature

Publication date:
2012

Document Version
Publisher's PDF, also known as Version of record

THE INFLUENCE OF NON-MAGNETOCALORIC PROPERTIES ON THE AMR PERFORMANCE

K.K. NIELSEN, C.R.H. BAHL, A. SMITH, K. ENGELBRECHT, U.L. OLSEN and N. PRYDS
Department of Energy Conversion and Storage, Technical University of Denmark
Frederiksborgvej 399, 4000-DK Roskilde, Denmark
+45 46774758, kaki@dtu.dk

ABSTRACT

The performance of Active Magnetic Regenerators (AMR) does not depend solely on the magnetocaloric effect of their constituents. Rather, it depends on several additional parameters, including, magnetic field, geometry (hydraulic diameter, cross-sectional area, regenerator length etc.), thermal properties (conductivity, specific heat and mass density) and operating parameters (utilization, frequency, number of transfer units etc.). In this paper we focus on the influence of three parameters on regenerator performance: 1) Solid thermal conductivity, 2) magnetostatic demagnetization and 3) flow maldistribution due to geometrically non-uniform regenerators.

It is shown that the AMR performance is optimal at an intermediate value of the solid thermal conductivity for many operating conditions. The magnetostatic demagnetization is shown to have a significant influence on the AMR performance, giving a strong dependence on the orientation of the applied field and the regenerator geometry. Finally, the flow maldistribution of non-uniform regenerator geometries is found to degrade the AMR performance even at minor deviations from perfectly homogeneous regenerator matrices.

1. INTRODUCTION

The performance of an active magnetic regenerator (AMR) is a function of a range of different physical effects. These include of course the magnetocaloric effect (MCE) of the solid refrigerant(s) used including the magnitude of the applied magnetic field. This has been investigated in numerous publications (Pecharsky and Gschneidner 2006, Engelbrecht and Bahl 2010, Smith et al 2012). Here, we will address three issues that have previously not been considered in (any) detail. These are the influence of the solid thermal conductivity (k_s), the effect of magnetostatic demagnetization and flow maldistribution due to non-uniform regenerator geometries.

The regenerator performance is typically expressed in terms of the number of transfer units (NTU) (Dragutinovic and Baclic 1998) defined as

$$NTU = \frac{hA_{HT}}{\dot{m}_f c_f}. \tag{1}$$

Here, the heat transfer coefficient between the solid and the fluid is denoted h, the heat transfer surface area is A_{HT}, the mass flow rate of the heat transfer fluid is $\dot{m}_f$ and the specific heat of the fluid is c_f. As the NTU increases the regenerator effectiveness generally increases also (Dragutinovic and Baclic, 1998). It is therefore evident from Eq. (1) that as the mass flow rate increases (at higher AMR operating frequencies, f) the heat transfer of the regenerator matrix must also increase to maintain a sufficient level of the NTU.

Another commonly used parameter describing the operating conditions of an AMR is the thermal utilization defined as

$$\varphi = \frac{\dot{m}_f c_f}{2 f m_s c_s}, \tag{2}$$

where the mass of the solid material is denoted m_s and the specific heat of the solid is c_s. The utilization describes the ratio between the thermal mass moved during the flow of the heat transfer fluid and the total thermal mass of the regenerator solid. The magnetization/demagnetization periods are assumed negligible in this definition.

2. MODELING

2.1. Numerical AMR models applied

Two numerical AMR models are applied in the following. One is a 1-dimensional model, described in detail in Engelbrecht (2008), which requires a Nusselt-number relation to describe the heat transfer interaction between the solid magnetocaloric material and the heat transfer fluid. The equations solved may be expressed as

$$(1-\varepsilon)\rho_s c_s \frac{\partial T_s}{\partial t} = \frac{\partial}{\partial x}\left(k_s \frac{\partial T_s}{\partial x}\right) + h a_s (T_f - T_s) - (1-\varepsilon)\rho_s T_s \frac{\partial s}{\partial H}\frac{\partial H}{\partial t} \tag{3}$$

$$\varepsilon \rho_f c_f \left(\frac{\partial T_f}{\partial t} + \tilde{u}\frac{\partial T_f}{\partial x}\right) = \frac{\partial T_f}{\partial x}\left(k_f \frac{\partial T_f}{\partial x}\right) + \varepsilon \left|\frac{\partial p}{\partial x}\bar{u}\right| - h a_s (T_f - T_s) \tag{4}$$

Here, the porosity, mass density, specific heat, temperature, time, thermal conductivity, heat transfer coefficient, specific surface area, specific entropy, magnetic field, mean flow velocity and pressure drop have been introduced and are denoted by ε, ρ, c, T, t, k, h, a_s, s, H, $\bar{u}$ and p, respectively. Subscripts s and f denote solid and fluid, respectively. The details of the numerical model are published in Engelbrecht (2008).

The other AMR model applied is 2-dimensional and published in Petersen et al. (2008) and Nielsen et al. (2009). It solves the coupled heat transfer equations for a flat plate regenerator in two dimensions and assumes a completely periodic regenerator, i.e. only half a plate and half a channel are spatially resolved. The equations solved may be written as

$$\rho_s c_s \frac{\partial T_s}{\partial t} = k_s \left(\frac{\partial^2 T_s}{\partial x^2} + \frac{\partial^2 T_s}{\partial y^2}\right) + \dot{Q}_{MCE} \tag{5}$$

$$\rho_f c_f \frac{\partial T_f}{\partial t} = k_f \left(\frac{\partial^2 T_f}{\partial x^2} + \frac{\partial^2 T_f}{\partial y^2}\right) - \rho_f c_f u_x \frac{\partial T_f}{\partial x}. \tag{6}$$

Here, the magnetocaloric effect (MCE) source term is denoted $\dot{Q}_{MCE}$. It is emphasized that the heat transfer is solved explicitly in both dimensions, which makes this model formulation suitable for, e.g., detailed studies of the influence of the solid thermal conductivity. However, in the 2D model it is not possible to adjust the heat transfer coefficient (describing the convective heat transfer between solid and fluid), which is possible in the 1D model. The two models therefore complement each other. Numerical and implementation details of the model may be found in Nielsen et al. (2009).

2.2. Solid thermal conductivity study

The thermal conductivity of the solid magnetocaloric regenerator material influences the AMR performance in two ways. Firstly, the heat transfer rate from the interior of the solid material to the heat transfer fluid should be as large as possible; indicating that a larger thermal conductivity transverse to the flow direction will result in increased AMR performance. Secondly, the fact that an AMR inherently has a temperature gradient in the direction of the flow (between the hot and cold sides) means that heat will flow through the regenerator from the hot to the cold side thus destroying the temperature gradient along the regenerator. This effect is a function of the temperature span (T_{hot}-T_{cold}), the length of the regenerator, L, and the thermal conductivity of the solid. This indicates that the conductivity in the flow direction should be minimized. From a thermal conduction point of view the optimal MCE is thus highly anisotropic; infinite conductivity in the direction perpendicular to the flow and zero conductivity in the flow or axial direction. In the absence of such anisotropic materials, an optimal value or a range of values that maximizes the AMR performance have to be found.

As the AMR operating frequency, f, is increased the cooling power density of the AMR device will increase as long as the *NTU* is sufficient for achieving regeneration. It may therefore be expected that the influence of axial conduction is reduced. It may also be expected that a longer regenerator is affected less by axial conduction than a shorter regenerator due to the increased conduction path in the former case for a fixed set of operating conditions. It is emphasized that the axial conduction is of main interest here and thus a single plate thickness is considered.

In the results section the AMR performance is presented as a function of the solid thermal conductivity at two different regenerator lengths (0.05 and 0.20 m, respectively) and at different AMR operating frequencies. The cooling power normalized to the maximum value is plotted at a fixed temperature span and thus higher values indicate better performance for otherwise fixed parameters. Naturally, the longer regenerator has more active magnetocaloric material and the cooling power has therefore been found on a per mass basis of the regenerator material in order to compare directly. It should be noted that the applied and internal fields during the AMR cycle are assumed equal and homogeneous thus disregarding any demagnetization effects. Finally, the MCE is modeled in a simplified manner such that the adiabatic temperature change is kept constant at 3 K, the specific heat in zero field is likewise constant (300 J/(kg·K)) and the in-field specific heat has been found through integration of the zero-field specific heat and the assumed adiabatic temperature change so that the MCE is thermodynamically self-consistent (Engelbrecht and Bahl, 2010). This removes any temperature-dependency in the adiabatic temperature change and the results thus reflect the direct impact on the performance from variation of the thermal conductivity. Table 1 provides details about the parameter space explored, and Table 2 shows the relevant materials properties input to the model.

Table 1: The geometric and operating parameters input to the thermal conductivity model. L is the length of the regenerator, H_f the channel thickness, H_s the plate thickness, f the AMR operating frequency, T_{cold} the cold-side temperatures, T_{hot} the hot side temperature and φ the utilization.

Parameter	L [m]	H_{f} [mm]	H_{s} [mm]	f [Hz]	T_{cold} [K]	T_{hot} [K]	φ [-]
Value	0.05, 0.20	0.2	0.3	0.25-4.0	265-295	295	0.5

Table 2: The thermal properties of the solid and the heat transfer fluid. k is the thermal conductivity, ρ the mass density and c the specific heat.

Property	k [W/m·K]	ρ [kg/m^3]	c [J/kg·K]
Solid	1-30	7900	300
Fluid	0.6	1000	4200

2.3. Magnetostatic demagnetization

It is well known that applying a homogeneous magnetic field to some structure made of ferromagnetic material results generally in an inhomogeneous internal field in the structure due to magnetostatic demagnetization (Joseph and Schloemann 1965, Smith et al. 2010). The internal field may be written as

$$\mathbf{H} = \mathbf{H}_{\mathrm{appl}} + \mathbf{H}_{\mathrm{dem}} \tag{7}$$

where the applied field is denoted $\mathbf{H}_{\mathrm{appl}}$ and the demagnetizing field is $\mathbf{H}_{\mathrm{dem}}$. The demagnetizing field is in general a function of the local internal field, $\mathbf{H}$, and the magnetization of the entire structure, $\mathbf{M}$. Many different established approaches exist in the literature for calculating $\mathbf{H}_{\mathrm{dem}}$ (Osborn 1945, Joseph and Schloemann 1965, Brug and Wolf 1985, Beleggia and De Graef 2003, Smith et al. 2010). Assuming that the magnetization locally at the point $\mathbf{r}$ is constant and discretizing the regenerator solid structure into rectangular prisms the demagnetizing field may be found through (Smith et al. 2010)

$$\mathbf{H}_{\mathrm{dem}}(\mathbf{r}) \approx -\sum_{i=1}^{n} \mathbf{N}(\mathbf{r}-\mathbf{r}_i)\cdot\mathbf{M}_0(\mathbf{r}_i, T_i, \mathbf{H}(\mathbf{r}_i, T_i)) \,. \tag{8}$$

Here, the temperature at the point $\mathbf{r}_i$ is denoted T_i and the demagnetization tensor field, $\mathbf{N}$, is found from basic magnetostatics (see Smith et al. (2010) for the components of $\mathbf{N}$). The summation in Eq. (8) is done over all the rectangular prisms the regenerator solid is discretized into (n is the number of prisms). For further details on the numerical implementation see Smith et al. (2010) and Christensen et al. (2011). Figure 1 shows a stack of plates, orientations of the applied field and the characteristic dimensions.

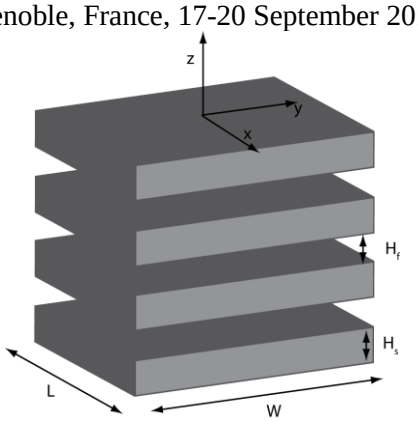

Figure 1: Geometry of stacked rectangular plates. The length in the flow direction is denoted *L*.

A reasonable connection between the magnetostatic demagnetization model and a numerical AMR model (as, e.g., described in Section 2.1) has not been implemented yet. In the following such a numerical scheme is described. In general, the two model types have different levels of detail and therefore also quite different solution times. It is not currently practical to solve the full demagnetization model alongside the temporal AMR model since one AMR cycle takes, on average, less than a minute to solve and the demagnetization models easily takes several hours to find the internal field especially when multiple magnetocaloric materials are considered and/or the effect of demagnetization is large. We therefore propose a scheme that is relatively simple, albeit still maintaining a fair amount of detail from the demagnetization model.

For a given parameter space, defined in terms of the geometric parameters N, L, W, H_s and H_f (see Figure 1 for details; N is the number of plates) and orientation of the applied field the model is used to calculate the internal field. It is then assumed that the following relation is a fair approximation to the internal field in the given parameter space:

$$H(x) = H_{appl} - K(x)M(T(x), H(x)) . \tag{9}$$

Here it is emphasized that the parameters refer to the magnitudes of the internal field, applied field and magnetization. $K(x)$ is defined as:

$$K(x) = \left\langle \frac{H_{appl} - H(x,y,z)}{M(T(x,y,z), H(x,y,z))} \right\rangle \Bigg|_{y,z} \tag{10}$$

The average is taken in the *yz*-plane at a given *x*. Once $K(x)$ has been found from the demagnetization model Eq. (9) is solved iteratively in the AMR model whenever the magnetic field is found. In this way the only extra input to the AMR model are $K(x)$ and $M(T,H)$. For the present study meanfield Gd is assumed with a Curie temperature, T_C, of 293 K. It was found that $K(x)$ is only a very weak function of the temperature span imposed on the demagnetization model. The magnitude of the applied field is in all cases 1 T.

Figure 2: Temperature distribution in a non-uniform stack of flat plates. The uneven channel thicknesses impose varying flow velocities in each channel since the pressure drop across each channel is identical.

2.4. Flow maldistribution

All AMR models published so far assume homogeneous regenerator geometries (i.e. a repeating cell is modeled). However, when constructing stacks of flat plates it is rarely the case that each plate and channel are perfectly identical. In fact, it has recently been found that a fair amount of variation in the channel thickness does occur within a given stack (Nielsen et al. 2012). The pressure drop across the regenerator will be virtually identical in each flow channel, resulting in different flow velocities in each individual channel depending on both the particular channel's thickness and the average channel thickness in the stack (Nielsen et al. 2012). Figure 2 illustrates this and it is apparent from the figure that thicker channels will have larger flow velocities than smaller channels due to the reduced flow resistance.

This effect results in a reduction of the regenerator performance, as found using the passive regenerator model published in (Jensen et al. 2010 and Nielsen et al. 2012). The regenerator performance for a particular (non-uniform) stack is found and reported as a reduction factor of the performance of an equivalent perfectly homogeneous stack. The convective heat transfer coefficient, h, is found through the well-known relation

$$Nu = \frac{hd_h}{k_f}, \tag{11}$$

where Nu is the Nusselt number and d_h is the hydraulic diameter. For parallel flat plates the Nusselt number, Nu_{pp}, may be found in Nickolay and Martin (2002).

It is a good approximation to state the non-uniform stack heat transfer performance as an equivalent ideal stack's performance reduced with a certain factor (Nielsen et al. 2012). The scaling of the Nusselt number is found as a function of Reynolds number (Re) for 50 stacks each having 20 plates (and channels) with thicknesses that are normally distributed with different standard deviations. The resulting Nusselt-Reynolds correlation may then be written as

$$Nu_{pp,stack} = C_{Nu}(\mathrm{Re})Nu_{pp}(\mathrm{Re}) \tag{12}$$

This relation is then used as input to the 1D model presented in Section 2.1 and the effect on the AMR performance is found as a reduction in cooling power at a given temperature span (and operating frequency and thermal utilization) compared to the case where C_{Nu} is equal to one (the homogeneous case).

Figure 3 shows an example of C_{Nu} as a function of Re for a stack of Gd plates with a thickness of 0.4 mm and nominal spacing (channel thickness) of 0.2 mm. The length is 40 mm. At low Re the maldistribution of flow is seen to yield a small C_{Nu} of the stack. As the Re increases this effect becomes smaller, however, that is simply due to the fact that the regenerator is overwhelmed with heat transfer fluid and the NTU becomes very small in any case.

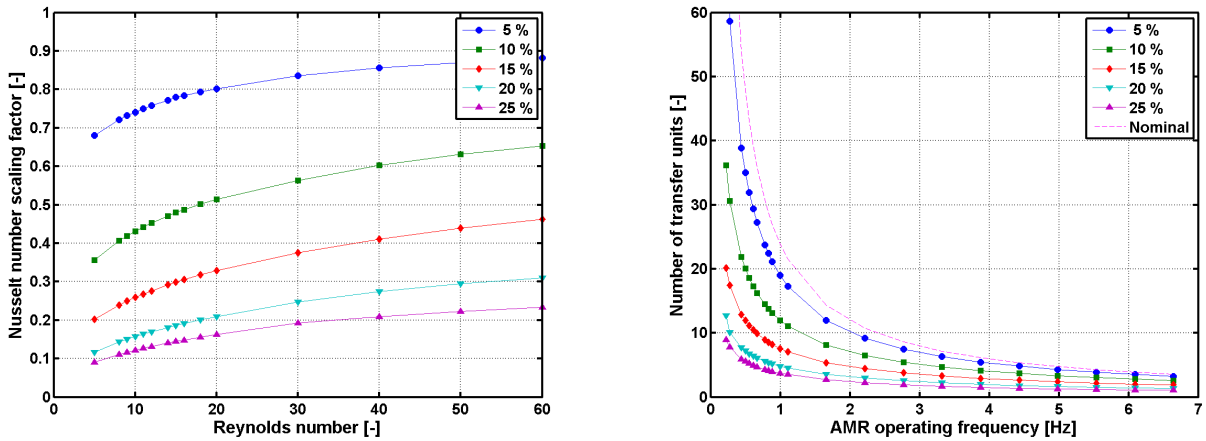

Figure 3: Left: the Nusselt scaling factor as a function of Reynolds number for five different standard deviations. Right: The resulting NTU as a function of AMR operating frequency for a thermal utilization of 0.5. The nominal curve indicates the NTU for a homogeneous stack.

3. RESULTS AND DISCUSSION

3.1. Solid thermal conductivity

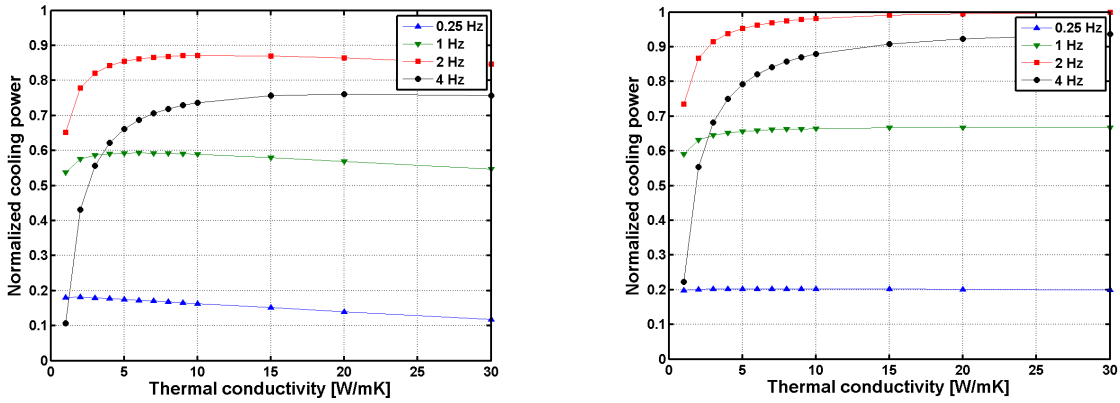

Figure 4: The normalized cooling power as a function of solid thermal conductivity at different AMR frequencies (indicated in the legend) at a utilization of 0.5 and a fixed temperature span of 10 K. Left: the regenerator is 50 mm long. Right: the regenerator is 200 mm long. The two plots may be compared directly since the cooling power has been found relative to the mass of the regenerator before being normalized to the maximum cooling power value in the aforementioned parameter space. The plots are based on data published in (Nielsen and Engelbrecht 2012).

The thermal conductivity of the solid was varied from 1 to 30 W/(m·K) and the cooling power found using the 2D model at different AMR frequencies, at a utilization of 0.5 and for a long (200 mm) and a short (50 mm) regenerator. The normalized cooling power is plotted in Figure 4. It is clear that at a low frequency the cooling power (at a fixed temperature span of 10 K) decreases linearly as a function of the thermal conductivity (in the short regenerator case) or remains virtually constant (in the long regenerator case).

As the AMR frequency is increased the cooling power is seen to be much more dependent on the thermal conductivity and it is clear that an optimum exists for the shorter regenerator, albeit depending on the AMR frequency, whereas for the longer regenerator the higher the thermal conductivity the larger the cooling power even though the benefit does become smaller above a conductivity of about 10 W/(m·K). This is due to the fact that the shorter regenerator is subjected to more axial conduction due to the shorter conduction path than is the case for the longer regenerator.

Another interesting result is that the longer regenerator generally yields a larger cooling power than the shorter one. That is also the result of the increased conduction path in the case of the longer regenerator. Finally, it should be noted that the largest cooling power, in both the short and long regenerator cases, is obtained at an AMR frequency of 2 Hz. The particular value is of course a result of the chosen geometry parameters; however, it is relevant to point out that at higher frequencies the performance decreases. This is due to the fact that the NTU becomes too small to sustain efficient regeneration (Dragutinovic and Baclic 1998). The influence of pressure drop is ignored in this study due to the fairly large channel thickness (Petersen et al. 2008).

3.2. Demagnetization

As described in Section 2.3 the magnetostatic demagnetization model and the 2D AMR model are combined in order to investigate the effect of geometric demagnetization on the AMR performance. Two stack configurations are considered. One is narrow (W=10 mm) the other wide (W=20 mm). See Figure 1 for reference. The narrow stack has 40 plates and the wide 20 plates thus both cases have the same mass. The regenerator length is 200 mm in both cases. The magnetic field is applied in two different directions: the y- and the z-direction. The former is generally expected to yield a smaller demagnetizing field than the latter.

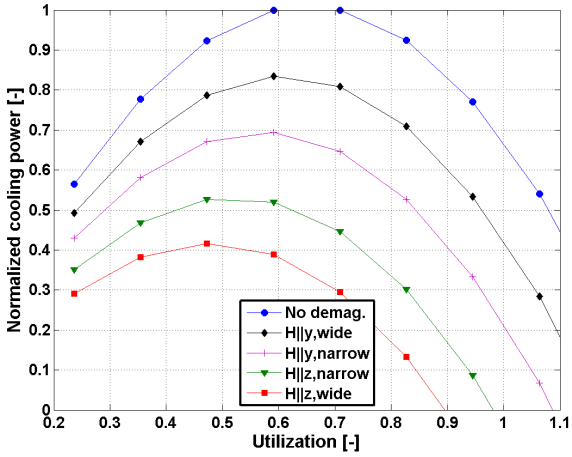

Figure 5: The normalized cooling power as function of utilization at a temperature span of 10 K. Four cases of the applied field and stack configuration are investigated (stack widths of 10 and 20 mm, respectively and the field along the *y*- and *z*-directions, respectively; see Figure 1).

In Figure 5 the normalized cooling power at a fixed temperature span of 10 K is given as a function of utilization for the four cases of different geometric demagnetization and a case without taking demagnetizing effects into account (i.e. $K(x)$=0 in Eq. (10)). It is obvious that neglecting demagnetization, the AMR model predicts a larger cooling power than when including the effect of demagnetization. It is also not surprising that the wide regenerator with the field along the *y*-direction is less affected by demagnetization while the wide regenerator with the field along the *z*-direction is most affected. The effect of demagnetization is in all cases significant, decreasing the maximum performance by 20-60%.

3.3. Flow maldistribution

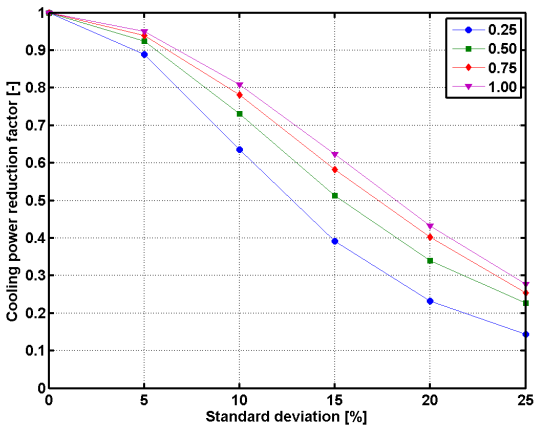

Figure 6: The reduction in cooling power as a function of standard deviation of the channel thickness of flat plate stacks for four values of the utilization (indicated in the legend) at a fixed temperature span of 10 K and AMR frequency of 2 Hz.

The Nu-Re scaling relation plotted in Figure 3 was applied in the 1D model using Eq. (12), H_s = 0.4 mm, H_f =0.2 mm and L=40 mm. Several AMR frequencies and utilizations were calculated and in Figure 6 the reduction in cooling power as a function of standard deviation of the channel thickness is shown for a frequency of 2 Hz, fixed temperature span of 10 K and four values of the utilization. As seen in Figure 6 the performance of the regenerator is very sensitive to the non-uniformity of the regenerator and as the standard deviation increases the AMR performance decreases. An increase in utilization reduces the effect of flow maldistribution (in this case), which is a result of a higher Reynolds number (see Figure 3).

4. CONCLUSION

Three different non-magnetocaloric aspects of the AMR were investigated with previously published numerical models. The influence of the thermal conductivity of the solid material was found to result in an optimal range of conductivities for maximizing the AMR cooling power.

The magnetostatic demagnetization was explored for different regenerator stack configurations and it was found that the impact of demagnetization on the AMR performance may be very large. It may therefore be concluded that it is important to be careful when designing an AMR device so as to minimize the demagnetizing effects.

The effect of flow maldistribution due to non-uniform flat plate stacks was found as a function of Reynolds number and distribution of flow channels. This was applied in an AMR model to probe the influence on the AMR performance and it was found that the impact may be significant at standard deviations of 10 % or more. Finally, it is concluded that these three effects each constrain the AMR design and that care should be taken when constructing AMRs with parallel plates and similar geometries. It is also noted that the results presented here are based on a limited parameter survey and that the conclusions may vary when other geometries and operating conditions are considered.

ACKNOWLEDGEMENTS

K.K. Nielsen wishes to thank The Danish Council for Independent Research | Technology and Production Sciences (Contract no. 10-092791) for financial support.

REFERENCES

[1] Beleggia, M. and De Graef, M. On the computation of the demagnetization tensor field for an arbitrary particle shape using Fourier space approach, 2003, *J. Mag. Mag. Mater*. 263, L1-L9

[2] Brug, J.A. and Wolf, W.P. Demagnetizing fields in magnetic measurements. I. Thin discs, *J. Appl. Phys*. 57 (10), 4685-4694 (1985)

[3] Christensen, D.V. Nielsen, K.K. Bahl, C.R.H. Smith, A. Demagnetizing effects in stacked rectangular prisms, *J. Phys. D: Appl. Phys.* 44 (21), 215004 (2011)

[4] Dragutinovic, G.D. and Baclic, B.S. *Operation of Counterflow Regenerators*, WIT press, Computational Mechanics Problems, Southampton, UK, 1998

[5] Engelbrecht, K. *A numerical model of an active magnetic regenerator refrigerator with experimental validation*, 2008, PhD thesis, University of Wisconsin-Madison.

[6] Engelbrecht, K. and Bahl, C.R.H. Evaluating the effect of magnetocaloric properties on magnetic refrigeration performance, 2010, *J. Appl. Phys.* 108, 123918

[7] Jensen, J.B. Engelbrecht, K. Bahl, C.R.H. Pryds, N. Nellis, G.F. Klein, S.A. Elmegaard, B. Modeling of parallel-plate regenerators with non-uniform plate distributions, 2010, *Int. J. Heat Mass Transfer* 53, 5065-5072

[8] Joseph, R.I. and Schloemann, E. Demagnetizing field in nonellipsoidal bodies, *J. Appl. Phys.* 36 (5), 1579-1593 (1965)

[9] Nickolay, M. and Martin, H. Improved approximation for the Nusselt number for hydrodynamically developed laminar flow between parallel plates, *Int. J. Heat Mass Transfer* 45, 3263-3266 (2002)

[10] Nielsen, K.K., Bahl, C.R.H., Smith, A., Bjørk, R. Pryds, N. and Hattel, J. Detailed numerical modeling of a linear parallel-plate Active Magnetic Regenerator, *Int. J. Refrig.* 32, 1478-1486 (2009)

[11] Nielsen, K.K., Engelbrecht, K. The influence of the solid thermal conductivity on active magnetic regenerators, 2012, *J. Phys. D: Appl. Phys.*, 45, 145001

[12] Nielsen, K.K., Engelbrecht, K., Christensen, D.V., Jensen, J.B., Smith, A. Bahl, C.R.H. Degradation of the performance of microchannel heat exchangers due to flow maldistribution, 2012, *Appl. Therm. Eng.* 40, 236-247

[13] Osborn, J.A. Demagnetizing factors of the general ellipsoid, *Phys. Rev*. 67, 351-357 (1945)

[14] Pecharsky, V.K. and Gschneidner, K.A. Advanced magnetocaloric materials: What does the future hold? 2006, *Int. J. of Refrig.* 29, 1239-1249

[15] Petersen, T.F., Pryds, N., Smith, A., Hattel, J., Schmidt, H., Knudsen, H.J.H. Two-dimensional mathematical model of a reciprocating room-temperature Active Magnetic Regenerator, 2008, *Int. J. Refrig*. 31, 432-443.

[16] Smith, A., Bahl, C.R.H., Bjørk, R., Engelbrecht, K., Nielsen, K.K., Pryds, N., Materials Challenges for high performance magnetocaloric refrigeration devices, 2012, *Adv. En. Mat.*, submitted

[17] Smith, A., Nielsen, K.K., Christensen, D.V., Bahl, C.R.H., Bjørk, R. and Hattel, J. The demagnetizing field of a non-uniform rectangular prism, *J. Appl. Phys.*, 107, 103910 (2010)